RAPID COMMUNICATIONS

PHYSICAL REVIEW A VOLUME 52, NUMBER 5 NOVEMBER 1995

Grid-free density-functional technique with analytical energy gradients

Katrina S. Werpetinski and Michael Cook
Department of Chemical Engineering, University of Massachusetts at Amherst, Amherst, Massachusetts 01003
(Received 21 February 1995)

We have implemented a completely analytical linear combination of atomic orbitals-$X\alpha$ local density-functional method with exact energy gradients. The superiority of the analytical method over the corresponding grid-based technique in terms of speed, smooth energy surfaces, and accurate gradients is demonstrated in calculations for the umbrella inversion mode of ammonia. The equilibrium geometry and inversion barrier height are also shown to compare well to experimental data.

PACS number(s): 31.15.Ew, 02.70.−c, 82.20.Wt

During the past 30 years, there has been a continual growth of interest in density-functional methods of electronic structure. These techniques are inherently faster than the classic *ab initio* methods, and recent calculational [1,2] and theoretical [3,4] studies have shown that density-functional techniques have an accuracy that is at least comparable to that of small configuration-interaction studies.

Since 1975 [5] a number of density-functional program packages have been developed that use a linear combination of atomic orbitals (LCAO) representation of the wave function. In principle, these codes should be capable of computing detailed energy surfaces, reactive pathways, and kinetics for large molecular systems; however, none of the current program packages has yet proved to be generally useful for these purposes.

There has been a great deal of recent progress in improving the accuracy of density-functional calculations for dissociation energies and activation energies through improvements to the form of the exchange-correlation functional [6]. However, a practical computational package for energy surfaces must possess other important features as well as accuracy. It should be computationally fast, it should produce smooth energy surfaces, and it should be able to calculate accurate energy gradients for the computed surface. In these areas, there is still much room for improvement.

The primary computational difficulty in density-functional techniques arises from the form of the exchange-correlation potential and energy. These involve, at a minimum, fractional powers of the electron density, such as $\rho^{1/3}$ and $\rho^{4/3}$. When the wave function and orbitals are expressed in many-center LCAO expansions, a fractional power of the charge density does not have a simple, closed form as a sum of separate terms. With few exceptions [7,8], all of the published LCAO density-functional algorithms address this problem by using a three-dimensional grid of points, either to perform the integrations involving the potential by numerical methods, or to fit the potential to a simpler functional form. Because the electron density decreases roughly exponentially away from the nuclear cusps, overlapping atom-centered grids are used almost universally.

The presence of a discrete grid will cause irregularities in an energy surface [9,10]. At each point on the surface, a "grid error" is introduced into the computed energy, and the size of this error varies as a function of geometry, producing "grid noise." Even when the grid error is small on an absolute scale, its variation can be rapid enough to cause significant distortions in the shape of an energy surface that varies by only a few kcal/mol. Grid noise can make it difficult to evaluate vibrational wave functions or kinetic parameters for a computed energy surface. The noise will also affect the energy gradients, reducing their usefulness for locating extrema.

At the simplest conceptual level, a very fine grid with a large number of points can be used to reduce the noise, but this is always at the expense of computational speed; and speed is one of the primary attractions of a density-functional approach. The development of techniques to decrease grid error while keeping the number of grid points moderate is an active research area [10–14]. These techniques include new grid quadratures, "adaptive" grids that check their own precision, and point-weighting schemes that attempt to create a smooth transition between grids centered on neighboring atoms.

The alternative is to develop analytical methods that eliminate the grid entirely. We have implemented a density-functional technique that requires no molecular grid and that includes analytical expressions for the calculation of energy gradients. This method gives smooth energy surfaces in a fraction of the computational time of a grid-based method. Because the gradients are exact, it is possible to locate extrema rapidly and efficiently.

The mathematical formalism for this method was originally developed by Dunlap [7,15]. The grid-based LCAO computer program package written by Mintmire was the starting point for our implementation [16].

Begin by assuming a $\rho^{1/3}$ form for the exchange potential:

$$V_{xc}=4/3\ C_\alpha \rho^{1/3}, \tag{1}$$

where

$$C_\alpha=-\left(\frac{9}{4}\alpha\right)\left(\frac{3}{8\pi}\right)^{1/3}. \tag{2}$$

For all the calculations reported here, α has been given the standard Gaspar-Kohn-Sham value of 2/3.

The functions $\rho^{1/3}$ and $\rho^{2/3}$ are fitted to sets of integrable, atom-centered functions:

$$\rho^{1/3} \approx \overline{\rho^{1/3}} = \sum_i a_i A_i , \tag{3}$$

$$(\overline{\rho^{1/3}})^2 \approx \overline{\rho^{2/3}} = \sum_i b_i B_i , \tag{4}$$

where an overbar denotes a fitted approximation to a quantity. In the present implementation, $\{A_i\}$ and $\{B_i\}$ are identical sets of Hermite Gaussian functions, although, in general, this is not required. Taylor expansions of the exchange energy to first order $\rho-(\overline{\rho^{1/3}})^3$ and $(\overline{\rho^{1/3}})^2-\overline{\rho^{2/3}}$ give the expression:

$$E_{xc}=\tfrac{4}{3}C_\alpha\langle\overline{\rho^{1/3}}\rho\rangle-\tfrac{2}{3}C_\alpha\langle\overline{\rho^{1/3}}\ \overline{\rho^{1/3}}\ \overline{\rho^{2/3}}\rangle+\tfrac{1}{3}C_\alpha\langle\overline{\rho^{2/3}}\ \overline{\rho^{2/3}}\rangle, \tag{5}$$

in which angle brackets indicate an integration over all space.

Variational minimization of the exchange energy with respect to the fitting coefficients $\{a_i\}$ and $\{b_i\}$ then gives the set of coupled, nonlinear equations

$$\langle A_i\rho\rangle-\sum_{j,k} a_j b_k\langle A_i A_j B_k\rangle=0, \tag{6}$$

$$\sum_{j,k} a_j a_k\langle A_j A_k B_i\rangle-\sum_j b_j\langle B_i B_j\rangle=0. \tag{7}$$

These equations are solved via the Newton-Raphson method to determine the fitting coefficients. Equations (6) and (7) involve at most three-center integrals, so that this is still an N^3 method. The particular form of Eqs. (6) and (7) depends on the $\rho^{1/3}$ form for the exchange potential; the addition of correlation corrections or nonlocal exchange-gradient terms would produce a more complicated set of nonlinear equations to solve.

Differentiating Eq. (5) with respect to the coordinates of nucleus A gives the gradients of the exchange energy as

$$\begin{aligned}\nabla_A E_{xc}=&\tfrac{4}{3}C_\alpha\sum_i a_i\nabla_A\langle A_i\rho\rangle\\&-\tfrac{2}{3}C_\alpha\sum_{i,j,k} a_i a_j b_k\nabla_A\langle A_i A_j B_k\rangle\\&+\tfrac{1}{3}C_\alpha\sum_{i,j} b_i b_j\nabla_A\langle B_i B_j\rangle.\end{aligned} \tag{8}$$

In contrast, the exchange energy and gradients of the exchange energy in the grid-based $X\alpha$ method are given by

$$E_{xc}=C_\alpha\langle\overline{\rho^{1/3}}\rho\rangle \tag{9}$$

and

$$\nabla_A E_{xc}=\tfrac{4}{3}C_\alpha\sum_i a_i\langle A_i\nabla_A\rho\rangle. \tag{10}$$

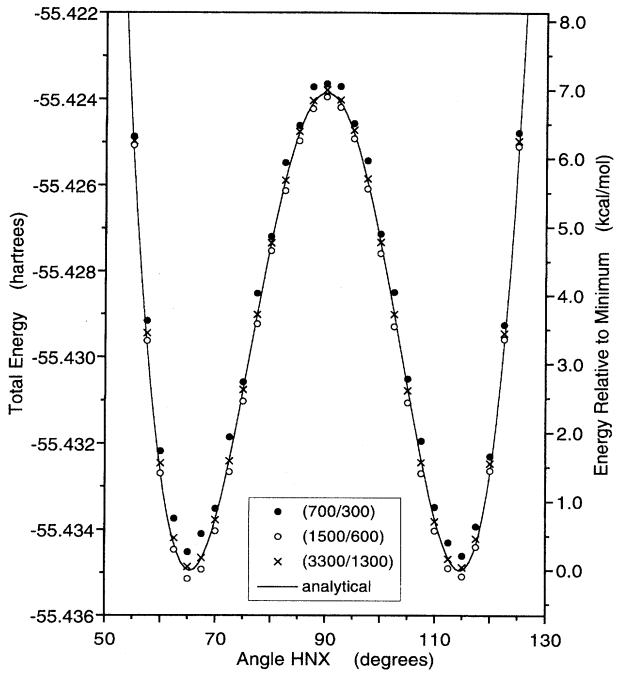

FIG. 1. Total energy of NH_3 as a function of the angle between the N—H bond and the threefold symmetry axis ($\angle$H—N—X). The N—H bond is held fixed at 1.0496 Å, the value obtained from a full analytical geometry optimization. All calculations were carried out using the 6-31G** basis set. The numbers in parentheses indicate the number of grid points in the form, ((number of points on N)/ (number of points on each H)).

The fit of $\rho^{1/3}$ is carried out numerically, and no fit of $\rho^{2/3}$ is performed.

We have used the umbrella inversion mode of ammonia to illustrate the performance of the analytical method as compared to that of the grid-based method. This inversion is a classic problem that has been studied by a wide variety of different theoretical techniques. Our atomic orbital basis is the 6-31G** basis set, with the slight modification of using a set of five d-type polarization functions rather than a set of six second-order functions. Two additional basis sets are used in the calculations, one for fitting the charge density in the Coulomb potential and the other for fitting $\rho^{1/3}$ and $\rho^{2/3}$ in the exchange energy. These two bases are comprised of uncontracted Hermite Gaussians. The charge-fitting (exchange-fitting) basis is derived from the orbital basis set by multiplying the exponent of each primitive Gaussian in the orbital basis by a factor of 2(2/3) to give the exponent for each uncontracted Gaussian of the same angular momentum in the charge-fitting (exchange-fitting) basis set. The only exception is that the set of five d-type orbital functions gives rise to a set of six second-order charge-fitting (exchange-fitting) functions.

Figure 1 illustrates the effect of grid noise. We report a range of three grid sizes denoted by ((number of points on N)/(number of points on each H)). These computations use pruned grids, in which the number of angular points in-

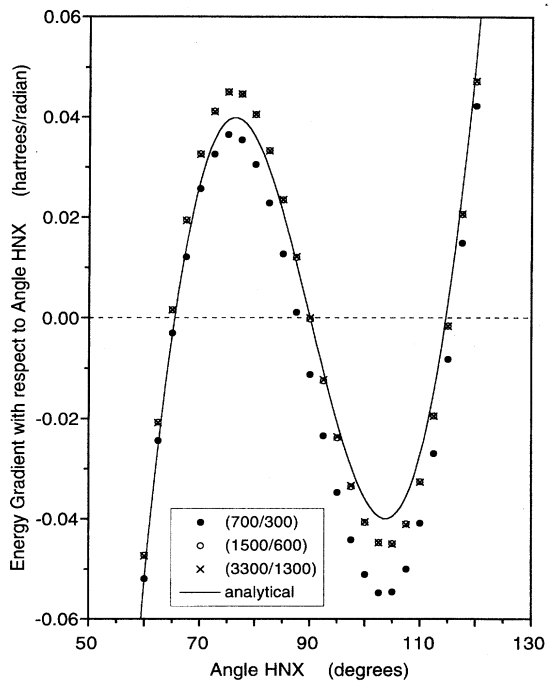

FIG. 2. Energy gradients of NH_3 with respect to $\angle$H— N—X, corresponding to the total energy calculations reported in Fig. 1. Note that the (3300/1300) and (1500/600) grids produce nearly identical gradients.

creases as a function of radius. The angular grid at each radius is rotated by a random angle, in order to reduce directional bias. Becke's fuzzy-weighting scheme is used [17].

The root-mean-square (rms) grid error in the smallest grid that we report in Fig. 1 is 0.25 kcal/mol. This is comparable to the error in the SG1 grid proposed as a standard by Gill *et al.* (0.2 kcal/mol) [10]. In our intermediate grid, the rms error is reduced to 0.13 kcal/mol; in the largest grid, 0.08 kcal/mol. Despite the small average size of these grid errors, the grid noise is still significant, particularly for the smallest grid. The severity of the noise depends not on the average grid error, but on the size and rapidity of the variation in that error as a function of geometry. The effect of grid noise on the energy surface would be more dramatic than this in larger and less symmetric species than NH_3.

The analytical calculations contain no grid noise, and are also faster than the grid-based technique. On a VAX 6400, a single point on the NH_3 energy surface requires approximately 110 s of CPU time for the analytical method versus 140, 240, or 420 s for the grid-based method using the (700/300), (1500/600), and (3300/1300) grids, respectively.

Figure 2 illustrates the difficulties with gradients in the grid-based method. The (700/300) gradients are useless for geometry optimization. They do not reflect the symmetry of the energy surface and do not vanish at the energy extrema. Much of this is the result of grid noise. The (1500/600) gradients are an improvement. They are nearly symmetric and vanish close to the energy extrema, however, they are not exact. The (3300/1300) and (1500/600) gradients are almost identical; the remaining errors in these gradients are due not to the grid, but rather to basis-set incompleteness.

The expression for the gradients in the grid-based method [Eq. (10)] is only exact in the limit of a complete exchange-fitting basis set. To the extent that this basis is incomplete, the computed gradients are not the true derivatives of the energy surface. In fact, when the basis set is incomplete, the gradients do not conserve linear and angular momentum; there are net forces and torques on the molecule. For the grid-based calculations in Fig. 2, these phantom forces have been calculated and removed from the gradients by subtraction. Several research groups who use numerical integration rather than fitting techniques have recently developed and implemented algorithms that rigorously conserve momentum by including appropriate correction terms [11–14]. However, some of these groups have cautioned that these terms can introduce additional numerical problems, particularly for smaller grids [13,14]. The gradients for the analytical method do not suffer from grid noise or basis-set incompleteness problems. They are exact derivatives of the computed energy surface.

For geometry optimization calculations using a standard gradient-minimization algorithm, the gradients from the grid-based calculations in Fig. 2 are of limited utility. The gradients from the analytical method, on the other hand, are very reliable. When the efficiency of optimizations is taken into account, the analytical technique is an order of magnitude or more faster than the grid-based method. For example, in optimizing the NH_3 geometry starting from an H—N—X angle of 105° and N—H bonds of 1.1 Å, the (3300/1300) grid requires 136 min of VAX 6400 CPU time to reach the energy minimum, while the analytical method requires only 13 min.

Our computed NH_3 geometry and inversion barrier compare well with the experimental values. We find the N—H bond=1.0496 Å and $\angle$H—N—X=114.7° compared to the experimental geometry, the N—H bond =1.0124 Å and $\angle$H—N—X=112.2° [18]. The inversion barrier found in Fig. 1 is 6.97 kcal/mol, but this surface has rigid N—H bonds. When the N—H bonds are allowed to relax during the inversion, the computed barrier is reduced to 6.16 kcal/mol, compared to the experimental value of 5.78 kcal/mol [19].

We are using the analytical $X\alpha$ technique described here to carry out a study of the torsional surfaces of the isoelectronic series, C_2H_6, N_2H_4, H_2O_2, which will be reported along with a more detailed description of the method in a future publication. Results to date suggest that the timing and smoothness advantages of the analytical technique over the grid-based method increase for these larger and less symmetric molecules.

Currently the most serious limitation on the analytical method is that the nonlinear equations (6) and (7) are restricted to $\rho^{1/3}$ potentials. A variety of correlation and nonlocal gradient correction terms are now often added to the basic $\rho^{1/3}$ potential [6], and these additional terms can be important, particularly for the quantitative description of bond dissociation energies [20]. It would be desirable to extend the present formalism to allow such terms to be incorporated in the exchange-correlation potential. In its present

form, we expect the method outlined here to have its most valuable applications in the description of conformational changes for which the net electron density gradients do not vary markedly [21], and in the initial rapid search of reactive energy surfaces to locate the positions of extrema and saddle points.

We would like to thank B. I. Dunlap, J. W. Mintmire, and C. T. White for helpful discussions and correspondence, and for their encouragement. We particularly thank John Mintmire for providing us with a copy of his grid-based LCAO program. This work was supported in part by UMass Faculty Research Grant No. 1-03360.

[1] A. D. Becke, J. Chem. Phys. **96**, 2155 (1992).
[2] R. M. Dickson and A. D. Becke, J. Chem. Phys. **99**, 3898 (1993).
[3] M. Cook and M. Karplus, J. Phys. Chem. **91**, 31 (1987).
[4] V. Tschinke and T. Ziegler, J. Chem. Phys. **93**, 8051 (1990).
[5] H. Sambe and R. H. Felton, J. Chem. Phys. **62**, 1122 (1975).
[6] A. D. Becke, Phys. Rev. A **38**, 3098 (1988).
[7] B. I. Dunlap, J. Phys. Chem. **90**, 5524 (1986).
[8] Y. C. Zheng and J. Almlöf, Chem. Phys. Lett. **214**, 397 (1993).
[9] B. I. Dunlap and M. Cook, Int. J. Quantum Chem. **29**, 767 (1986).
[10] P. M. W. Gill, B. G. Johnson, and J. A. Pople, Chem. Phys. Lett. **209**, 506 (1993).
[11] B. G. Johnson and M. J. Frisch, Chem. Phys. Lett. **216**, 133 (1993).
[12] B. G. Johnson, P. M. W. Gill, and J. A. Pople, Chem. Phys. Lett. **220**, 377 (1994).
[13] J. Baker, J. Andzelm, A. Scheiner, and B. Delley, J. Chem. Phys. **101**, 8894 (1994).
[14] N. C. Handy, D. J. Tozer, G. J. Laming, R. W. Murray, and R. D. Amos, Israel J. Chem. **33**, 331 (1993).
[15] B. I. Dunlap and N. Rösch, J. Chim. Phys. **86**, 671 (1989).
[16] J. W. Mintmire, Int. J. Quantum Chem. Symp. **24**, 851 (1990).
[17] A. D. Becke, J. Chem. Phys. **88**, 2547 (1988).
[18] W. S. Benedict and E. K. Plyler, Can. J. Phys. **35**, 1235 (1957).
[19] J. D. Swalen and J. A. Ibers, J. Chem. Phys. **36**, 1914 (1962).
[20] A. D. Becke, J. Chem. Phys. **96**, 2155 (1992).
[21] T. Ziegler, Chem. Rev. **91**, 651 (1991).